Relative Quantification of Proteins in Formalin-Fixed Paraffin-Embedded Breast Cancer Tissue Using Multiplexed Mass Spectrometry Assays

Authors

Carine Steiner, Pierre Lescuyer, Paul Cutler, Jean-Christophe Tille, and Axel Ducret

Correspondence

carine.steiner@gmail.com

Graphical Abstract

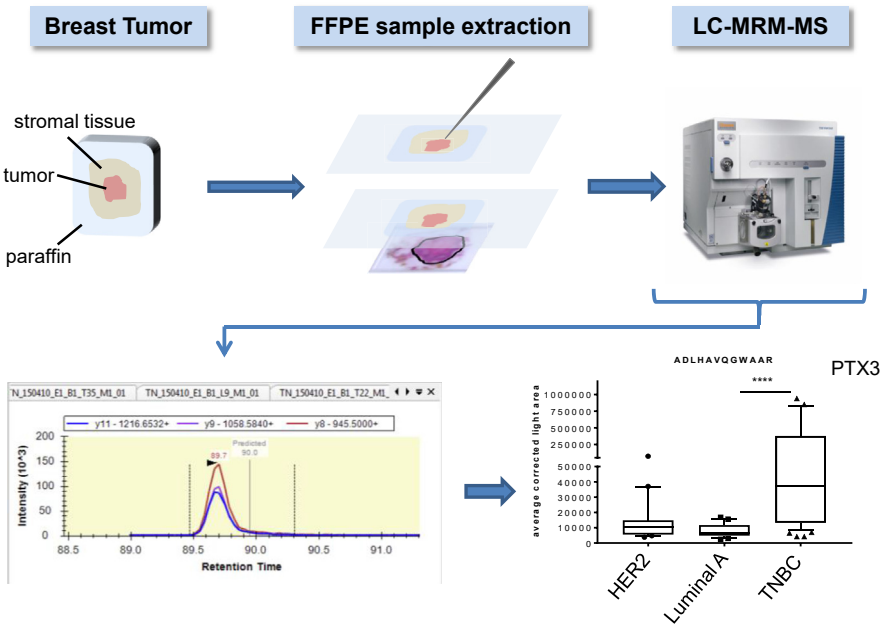

In Brief

The identification of biomarkers is an important challenge in oncology. In this study, we developed a liquid chromatography coupled to multiple reaction monitoring mass spectrometry assay that allows measuring the expression of target proteins in formalin-fixed paraffin-embedded tumor samples, the standard method for biopsy storage in clinical pathology. The method provided quantitative information on 185 proteins from three groups of breast tumors: triple-negative, HER2-overexpressing, and luminal A. In addition to markers such as HER2 or hormone receptors, we identified several proteins which are expressed differentially in triple-negative breast cancer samples.

Highlights

- Tier 2 MRM assay for relative protein quantification in tissue samples.
- Targeted analysis of 185 breast cancer–related proteins.
- Comparative proteomic analysis of formalin-fixed paraffin-embedded tumor samples.
- Analysis of luminal A, HER2-overexpressing, and triple negative breast tumors.

2022, Mol Cell Proteomics *21*(*11*), 100416
© 2022 THE AUTHORS. Published by Elsevier Inc on behalf of American Society for Biochemistry and Molecular Biology. This is an open access article under the CC BY-NC-ND license (http://creativecommons.org/licenses/by-nc-nd/4.0/).
https://doi.org/10.1016/j.mcpro.2022.100416

Relative Quantification of Proteins in Formalin-Fixed Paraffin-Embedded Breast Cancer Tissue Using Multiplexed Mass Spectrometry Assays

Carine Steiner[1,2,*], Pierre Lescuyer[1,3], Paul Cutler[2], Jean-Christophe Tille[4], and Axel Ducret[2]

The identification of clinically relevant biomarkers represents an important challenge in oncology. This problem can be addressed with biomarker discovery and verification studies performed directly in tumor samples using formalin-fixed paraffin-embedded (FFPE) tissues. However, reliably measuring proteins in FFPE samples remains challenging. Here, we demonstrate the use of liquid chromatography coupled to multiple reaction monitoring mass spectrometry (LC-MRM/MS) as an effective technique for such applications. An LC-MRM/MS method was developed to simultaneously quantify hundreds of peptides extracted from FFPE samples and was applied to the targeted measurement of 200 proteins in 48 triple-negative, 19 HER2-overexpressing, and 20 luminal A breast tumors. Quantitative information was obtained for 185 proteins, including known markers of breast cancer such as HER2, hormone receptors, Ki-67, or inflammation-related proteins. LC-MRM/MS results for these proteins matched immunohistochemistry or chromogenic *in situ* hybridization data. In addition, comparison of our results with data from the literature showed that several proteins representing potential biomarkers were identified as differentially expressed in triple-negative breast cancer samples. These results indicate that LC-MRM/MS assays can reliably measure large sets of proteins using the analysis of surrogate peptides extracted from FFPE samples. This approach allows to simultaneously quantify the expression of target proteins from various pathways in tumor samples. LC-MRM/MS is thus a powerful tool for the relative quantification of proteins in FFPE tissues and for biomarker discovery.

The identification of clinically relevant biomarkers represents an important challenge for multifactorial diseases such as cancer (1–4). While biomarkers are often assessed in blood or urine to avoid invasive sample collection, cancer biomarkers are preferably measured in tissue samples to maximize sensitivity and specificity. Confirmation of diagnosis and molecular characterization of tumors are indeed routinely performed on biopsies, thereby making tissues the samples of choice for cancer biomarker discovery (5). In this context, one of the critical factors for the discovery and validation of new biomarkers is the access to a large number of tissue samples representative of the disease. In clinical practice, most tissue specimens are formalin-fixed and paraffin-embedded (FFPE) since this process stabilizes the sample and allows storage at room temperature for years. Consequently, FFPE tissue samples are more readily available than fresh frozen samples. Importantly, FFPE tissue samples are commonly associated with reliable clinical information, such as patient demographics, disease stage, and comorbidities. As of today, analysis of proteins in FFPE tissues mainly relies on immunohistochemistry (IHC). However, development of novel IHC assays is challenging due to the requirement for highly specific antibodies. Also, IHC affords only limited possibilities for multiplexing, which strongly restricts its use for biomarker discovery approaches.

Proteins in FFPE tissues were long thought to be inaccessible to mass spectrometry (MS) analysis due to the cross-links formed during formalin fixation. However, over the past years, several groups have demonstrated the possibility to

From the [1]Division of Laboratory Medicine, Diagnostic Department, Geneva University Hospitals, Geneva, Switzerland; [2]BiOmics and Pathology, Pharmaceutical Sciences, Roche Pharma Research & Early Development (pRED), Roche Innovation Center Basel, Switzerland; [3]Department of Medical Specialties, Faculty of Medicine, University of Geneva, Geneva, Switzerland; [4]Division of Clinical Pathology, Diagnostic Department, Geneva University Hospitals, Geneva, Switzerland

*For correspondence: Carine Steiner, carine.steiner@gmail.com.

Present address for Carine Steiner: Analytical Research & Development, Pharma Technical Development, F. Hoffmann-La Roche, Basel, Switzerland.

Present address for Paul Cutler: Development Sciences, UCB Pharma, Slough, United Kingdom.

© 2022 THE AUTHORS. Published by Elsevier Inc on behalf of American Society for Biochemistry and Molecular Biology.
This is an open access article under the CC BY-NC-ND license (http://creativecommons.org/licenses/by-nc-nd/4.0/).

https://doi.org/10.1016/j.mcpro.2022.100416

reverse formalin cross-links and thereby to extract proteins from FFPE tissue samples (6, 7). Studies using MS workflows then demonstrated that proteomes retrieved from matched FFPE and frozen tissues were highly similar (8, 9). Finally, several studies used targeted MS assays based on multiple reaction monitoring (MRM) to measure relative protein abundance in FFPE tissues (10–14). These measurements showed a high agreement with IHC. Moreover, one of the most appealing aspects of a targeted MS approach is the enabling of highly multiplexed assays for the concurrent measurement of up to hundreds of selected proteins in a given sample.

The use of heavy-labeled peptides as internal standards for each analyte also ensures a reliable comparison of protein levels between multiple samples.

In this study, we investigated the potential of a targeted MS approach for the relative quantification of preselected protein panels in FFPE triple-negative breast cancer (TNBC) tissue samples. TNBC represents 12 to 17% of all breast cancer cases (15, 16). They are defined by the lack of HER2 overexpression and by the absence of estrogen receptor (ER) and progesterone receptor (PR) expression (17, 18). TNBC mostly affect young women (17, 19) and represent a major clinical challenge due to their aggressiveness and poor prognosis. Surgery and chemotherapy are currently the main treatment options as these tumors are unresponsive to targeted therapies, such as trastuzumab or hormone receptor modulators (20–22). In addition, TNBC represents a heterogeneous group of diseases in terms of pathological features, mutations, and gene expression profiles (23). TNBC is of high interest for biomarker discovery since there is to date no generally accepted diagnostic marker for these tumors. In this study, we describe the development of two multiplexed MRM assays for the simultaneous measurement of 200 proteins with potential implication in TNBC pathobiology. The MRM assays were applied on FFPE samples from 48 TNBC tumors and 39 non-TNBC tumors (19 cases of HER2 overexpressing breast cancers and 20 cases of luminal A breast cancers). Data comparison between these sample groups confirmed known molecular features, such as HER2 overexpression in the HER2 overexpressing breast cancers. Differential expression of potential TNBC-associated protein markers was also highlighted, underlying the potential of the approach for biomarker discovery. Verification experiments by IHC were performed for the following proteins: epidermal growth factor receptor (EGFR), cytokeratin (CK) 5/6, CK14, androgen receptor (AR), CD20, CD3, CD8, CD4, and CD68. In addition, HER2 expression was determined by chromogenic *in situ* hybridization (CISH).

EXPERIMENTAL PROCEDURES

Experimental Design and Statistical Rationale

Two MRM assays were developed for 200 proteins relevant to the TNBC phenotype. To evaluate the applicability of the developed methods on real clinical samples, the proteins were measured in a cohort of 90 breast cancer FFPE tissue samples (50 cases of TNBC, 20 cases of luminal A breast cancers, and 20 cases of HER2 overexpressing breast cancers) obtained from the Clinical Pathology Division of the Geneva University Hospitals. All samples were analyzed in duplicate (adjacent FFPE tissue slices processed separately). The samples were randomized three times throughout the analytical process (prior to tumor dissection, prior to peptide extraction, and again prior to LC-MRM/MS analysis). The samples were not blinded.

FFPE Tissue Samples

The study was approved by the ethical committee for research of the Canton of Geneva (protocol NAC 13–109) and abides by the Declaration of Helsinki principles. FFPE samples from breast tumor resections were selected retrospectively from the archives of the Division of Clinical Pathology of the Geneva University Hospitals on the period 2001 to 2011. All samples corresponded to cases of lumpectomy or mastectomy from neo-adjuvant treatment-naïve women with invasive breast carcinomas. Exclusion criteria were male gender and administration of a neo-adjuvant treatment. The cohort included 50 cases of TNBC, 20 cases of luminal A breast cancers, and 20 cases of HER2 overexpressing breast cancers (supplemental Table S1). ER, PR, proliferation marker protein Ki-67 (Ki-67) expression, and HER2 amplification status were available for all samples. TNBC cases were defined by the absence of ER and PR expression as well as the absence of HER2 amplification determined by a CISH ratio HER2/CEP17 below 2. Luminal A tumors were characterized by the expression of ER, PR, and a Ki-67 proliferation index under 20%. HER2 amplified tumors were characterized by a CISH ratio HER2/CEP17 above 2. This group included both HER2 breast tumors (ER and PR negative) and HER2-positive luminal B tumors (ER and/or PR positive, high levels of Ki-67). In the context of methodology development, the number of samples is not as critical as in biomarker discovery and validation studies. We therefore did not use statistics for sample size calculation. We tried to obtain as many samples as possible from the clinical pathology division of our hospital. We thus empirically collected 90 tumor tissue samples distributed in three groups of breast cancer subtypes. This represents to our opinion a sufficient number of samples for the proof of concept.

From the 50 TNBC samples that were originally selected, two samples (T20 and T28) were excluded from the data analysis. The first sample had been misclassified as triple-negative whereas it was a luminal A sample. The second sample was removed because the tumor area was significantly different between the first and the last control hematoxylin and eosin (H&E) slides, and therefore the measured surface did not correspond to the surface extracted for protein analysis. Moreover, one of the HER2 samples (H5) is missing in replicate 1 because the sample was accidently lost during sample preparation.

Peptides Extraction From FFPE Tissue

Paraffin blocks containing the resected tumors were cut using a microtome according to the following scheme: 10 4 μm thick slices, followed by six 10 μm slices and finally one last 4 μm slice were cut and mounted on SuperFrost glass slides (Thermo Fisher Scientific). The first and the last 4 μm thick slices were H&E stained in order to confirm the presence of tumor tissue throughout all collected tissue slices. The remaining 4 μm slices were stored at –20 °C for further IHC analyses. The 10 μm tissue slices were used for peptide extraction (2 slices per replicate and two backup slices). The infiltrative tumor area, omitting ductal or lobular *in situ* carcinoma, was delimited on the first H&E slide by a trained clinical pathologist. The surface tumor area was measured using the Pannoramic Viewer software (3DHistech) on the H&E template slides, which were digitally scanned using the

Pannoramic 250 Flash II scanner (3DHistech). Tumor slice surfaces ranged from 5 mm^2 to 350 mm^2 (supplemental Table S1). The percentage of tumor cells in the tumor area was determined by a trained pathologist (supplemental Table S1). Scalpel macrodissection of the tumor area was performed by superimposing the 10 μm slices with the H&E template. The dissected tumor FFPE tissue was deparaffinated and rehydrated using a series of UltraClear (Biosystems Switzerland AG) and graded alcohol baths, after which the rehydrated tissue was collected with a needle and stored at −80 °C until peptide extraction. A detailed protocol for the extraction of peptides from FFPE tissue slices was published previously (13). Briefly, tissue recovered from two 10 μm tissue slices was suspended in 100 μl of 20 mM Tris-HCl buffer, pH 8.5 containing 1 % (w/v) RapiGest SF and 25 μg 1,4-dithioerythritol. The tube was heated at 100 °C for 20 min and sonicated. The sample was heated again at 80 °C for 2 h, after which it underwent a second round of sonication and was subjected to alkylation by adding 25 μl of a 40 mM ammonium bicarbonate solution containing 125 μg iodoacetamide. Digestion was performed overnight at 37 °C using 2 μg of sequencing grade modified trypsin (Promega). The sample was then acidified and desalted, after which the eluate was evaporated to dryness using a speed-vac concentrator. The extract was kept at −20 °C until use. Because of the large number of samples, tissue extracts were processed in separate batches of 20 to 30. Randomization was performed prior to tumor dissection, prior to peptide extraction, and again prior to LC-MRM/MS analysis, using the randomize function in Excel. All FFPE tissue samples were extracted and analyzed in duplicate (from two independent adjacent tissue slices).

MRM Assay Development

An MRM assay was developed for 224 proteins, which had been described as of interest for TNBC and/or basal-like breast cancer by gene expression and proteomics studies (24–30) (supplemental Table S2). A detailed protocol for candidate proteins and peptide selection was published previously (31). Briefly, the development process included *in silico* analyses of the selected proteins using the Skyline software (version 3.1, MacCoss Lab Software) combined with a prediction tool (32) to determine peptides with the highest probability of detection by MS. Crude analogs of the selected peptides labeled at the C-terminal side using [U-13C6; U-15N4] Arg or [U-13C6; U-15N2] Lys were used as internal standards (JPT Peptide Technologies) and were used throughout the full study. These peptides were solubilized in 2% acetonitrile, 0.1% formic acid and were analyzed on a Q Exactive mass spectrometer (Thermo Fisher Scientific) to ensure that the correct sequences had been synthesized and that the desired products were among the dominant species. The data were searched using Mascot (version 2.5.0, Matrix Science Ltd) against the human Uniprot protein database (accessed on 13.02.2014, containing 23′592 reviewed entries), and the search results were exported in Skyline to generate a spectral library. Using Skyline, 124 unscheduled MS methods were generated to screen the corresponding >19,000 transitions on a TSQ Vantage triple-quadrupole mass spectrometer (Thermo Fisher Scientific). The obtained data were reviewed in Skyline, and the five most intense transitions were selected for each precursor. In a third step, labeled peptides were spiked in a biological matrix prepared by mixing tryptic digests of five basal-like breast cancer cell lines previously fixed with formalin. This sample was used to look for possible matrix-related analytical interferences and further refine MS parameters. In the last screening round, sequential dilutions of the selected peptides in the biological matrix were analyzed to check for response linearity in the mass spectrometer. The final MRM assay comprised 200 proteins, which were distributed among two different acquisition methods to allow the measurement of the corresponding 480 peptides with 2880 transitions for the endogenous peptides and the heavy-labeled internal standards (supplemental Table S3). In the final method, we used indexed retention time peptides (33) and the *intelligent SRM* feature available on the TSQ Vantage (34, 35) to perform dynamic scheduling and to compensate for retention time shifts. A set of 12 peptides was selected from the synthetic peptides pool and used as reference indexed retention time peptides.

LC-MRM/MS Analysis

In a previous study (13), we determined that a 20 μm thick FFPE tissue sample contains approximately 1 μg protein/mm^2. Based on this estimation, each sample extract was reconstituted in an appropriate volume of mobile phase A (2% acetonitrile, 0.1% formic acid) in order to reach a concentration of 400 ng/μl total protein. This sample solution was further mixed in a 1:1 ratio with the internal standard solution containing 10 fmol/μl of each heavy-labeled internal standard in mobile phase A. The resulting sample solution contained 200 ng/μl of total protein as well as 5 fmol/μl of each of the heavy-labeled internal standard. A volume of 5 μl was injected into the LC-MS system for MRM analysis. Extracts from FFPE tissue samples were analyzed by MRM on a TSQ Vantage mass spectrometer (Thermo Fisher Scientific) equipped with a Dionex Ultimate 3000 RSLCnano system (Thermo Fisher Scientific). Peptides were separated on a 75 μm × 50 cm EasySpray column (PepMap RSLC, C18, 2 μm, 100 Å; Thermo Fisher Scientific) with a 100 μm × 2 cm precolumn (Acclaim PepMap 100, C18, 5 μm, 100 Å; Thermo Fisher Scientific). The analytical separation was run using a gradient of mobile phase A (0.1 % formic acid, 2 % acetonitrile) and mobile phase B (0.1 % formic acid in acetonitrile) as follows: 2% to 30% B in 90 min, 30% to 60% B in 6 min, and 60% to 80% B in 2 min at a flow rate of 250 nl/min. The spray voltage was set to 2600 V, the ion transfer capillary temperature was set to 240 °C, the resolution was set to 0.7 Th for Q1 and Q3 (FWHM), and the collision gas pressure was set at 1.5 mTorr. LC-MRM/MS runs were performed with 3 min acquisition windows. Cycle time was set to 2.0 s with a maximum of 200 concomitant transitions measured, thereby ensuring a minimum dwell time of 10 ms per transition. Collision energy was set using the following linear equation embedded in Skyline: CE = slope * (precursor m/z) + intercept. This equation is instrument specific, and each charge state of the precursor, namely 2+ and 3+, is allowed to have a different equation (36). The equation parameters were for 2+ precursors: slope: 0.030, intercept: 2.905, and for 3+ precursors: slope: 0.038, intercept: 2.281. These values were the same for all peptides.

A QC sample prepared by mixing an equal amount of 20 FFPE tissue extracts from the first extraction batch was analyzed and processed together with the clinical samples. This QC sample was injected several times in each batch of clinical samples and equally distributed throughout the sequence.

MRM Data Processing

MRM data were imported in Skyline where peaks were integrated automatically. In order to facilitate data review, a reference chromatogram library was built in Panorama (37) using MRM data from previous analysis of heavy-labeled standard peptides in 2% acetonitrile, 0.1% formic acid on a TSQ Vantage. This reference library was loaded in Skyline and used to assess peak integration in MRM analysis using the dot product (dotp) function. Each peptide was manually reviewed throughout all samples, and if necessary, the integration was corrected based on the elution time, the transition ratio of the heavy-labeled internal standard, and the match with the chromatogram library (dotp). Peaks which had partly shifted outside of the acquisition window were removed if less than 60% of the peak was visible (visual evaluation). In addition, peptides for which the endogenous trace could not be distinguished from the noise or for which the correct peak could not be identified with sufficient confidence were flagged.

Peak areas of the fragments monitored for a given peptide were summed. Summed peak areas were exported to Tibco Spotfire (version 5.5, TIBCO Software Inc.) for further processing and normalization to the internal standard. Summed light peak areas were corrected for variation due to the LC-MS analysis using the area of the heavy peptides according to the following equation:

$$L_{norm\ ps} = \frac{L_{ps} * \overline{X}_p}{X_{ps}}$$

where *Lnorm ps* is the light area for peptide *p* in sample *s* after normalization for internal standard, *Lps i*s the light area for peptide *p* in sample *s*, $\overline{X}p$ is the median heavy peak area for a given peptide in all samples, and *Xps* is the heavy peak area for peptide *p* in sample *s* (38). MRM data were also normalized by the percentage of tumor content. Both data, with and without normalization for tumor content, were used for further analysis. MRM and normalization data can be found in supplemental Table S4.

IHC and In Situ Hybridization

HER2 expression was determined for all tumors by CISH using Ventana HER2 Dual ISH DNA Probe Cocktail (Roche Diagnostics). Moreover, several proteins were assessed by IHC: EGFR (ref. 280005, Invitrogen - Thermo Fisher Scientific), CK 5/6 (ref. M7237, Dako Agilent), CK14 (ref. 314M-16, Cell Marque), AR (ref. AB108341, Abcam), CD20 (ref. NCL-L-CD20-L26, Novocastra, Biosystems), CD3 (ref. 790-4460, Roche Diagnostics,), CD8 (ref M7103, Dako Agilent), CD4 (ref. 104R-16, Cell Marque), and CD68 (ref. M0876, Dako Agilent). CISH and IHC were performed with antigen retrieval on a Ventana Benchmark XT automated stainer (Roche Diagnostics). The intensity of IHC reactions was evaluated using the Remmele immunoreactive score.

Statistical Analysis

Statistical tests were performed using Graphpad Prism (version 7, GraphPad Software). Box plots show the median as well as the 25th and 75th percentiles. Whiskers show the 10th and 90th percentiles. We used nonparametric statistical methods since we had relatively small sample groups with non-Gaussian distribution. Peptide levels between tumor groups were compared using the nonparametric Kruskal–Wallis test, followed by Dunn's multiple comparison test (testing each pair of groups for a given peptide; alpha = 0.05). The adjusted *p*-value was reported for each test. In addition, the significance level of 0.05 was adapted according to Bonferroni's correction for multiple testing. The alpha value 0.05 was divided by the number of peptides tested (n = 71) leading to an adjusted significance level of 0.0007 (tests returning a *p*-value lower than 0.0007 are considered to be significantly different). Correlations were calculated using the Spearman rank correlation test (two-tailed, alpha = 0.05).

RESULTS

LC-MRM/MS Assay

In total, 315 peptides in replicate 1 and 404 peptides in replicate two were considered to have a valid MS signal. As a result, 185 proteins from the 200 in the assay (>90%) could be quantified in either one or both replicates. CVs were calculated for all measured peptides using the QC sample repeatedly injected during each LC-MRM/MS sequence (supplemental Table S5). As seen in Fig. 1*A*, more than half of the peptides had a CV below 20% in both replicates. After exclusion of peptides with a poor quality signal, the proportion of peptides with a CV below 20% was 76% (238/315 peptides) in replicate 1 and 66% (265/404 peptides) in replicate 2. Not surprisingly, there was a clear negative correlation between the MS signal intensity and the CV value for a given peptide as shown in Fig. 1*B*.

Markers Used in Clinic for Breast Tumor Classification

Data from proteins which are routinely assessed in clinical pathology for breast tumor classification were used to evaluate the reliability of MRM assay measurements. MS results obtained for peptides corresponding to HER2 (ERBB2), ER (ESR1), and PR (PRGR) were showed to match the expected protein expression pattern according to the breast cancer subtype. (Figs. 2, *A*, *B* and S1). In TNBC samples, very low levels of HER2, ESR1, and PRGR peptides were detected. In the luminal A group, ESR1 and PRGR peptides were expressed at high levels while HER2 peptides were measured at low concentrations. Finally, in the group of HER2-amplified tumors, a clear pattern of HER2 overexpression was confirmed compared to TNBC and luminal A samples. This group of HER2 overexpressing tumors actually comprised two subgroups: HER2 tumors as well as HER2 positive luminal B tumors. Luminal B tumors differ from strictly speaking HER2 tumors because they are hormone receptor-positive (*i.e.*, they express ESR1 and/or PRGR). This explains the range of abundances measured for ESR1 and PRGR peptides in the HER2-amplified tumor group (Figs. 2, *A*, *B* and S1). Further analysis of these two subgroups confirmed that ESR1 and PRGR peptides were measured at much higher levels in luminal B samples compared to HER2 tumors (Figs. 3, *A*, *B* and S2). Luminal B tumors represent a type of breast cancer that differs from luminal A tumors by showing higher expression levels of the proliferation marker Ki-67. Ki-67 is routinely measured for breast tumor characterization as it is an important marker for predicting the prognosis of luminal breast cancer (39). The MRM data generated here show that luminal B tumors can be separated from luminal A tumors based on the Ki-67 AQALEDLAGFK peptide level (Fig. 4*A*). Comparison of MRM data for Ki-67 with protein expression measurements by IHC showed a positive correlation (Fig. 4*B*). Data significance decreased however after normalization for tumor content (Fig. 4, *C* and *D*). The correlation between IHC results and MRM data was not determined for ER and PR since the distribution of IHC scores for these proteins was binary with almost all values being either zero or eight and very few cases having an intermediate score. It is noteworthy that a second member of the estrogen receptor family, ESR2, was also included in the MRM assay. However, the two corresponding peptides were not detected in breast tumor extracts. This result was coherent with data from the Human Protein Atlas database (https://www.proteinatlas.org/ENSG00000140009-ESR2/tissue, accessed 17.07.2020) which indicates that in

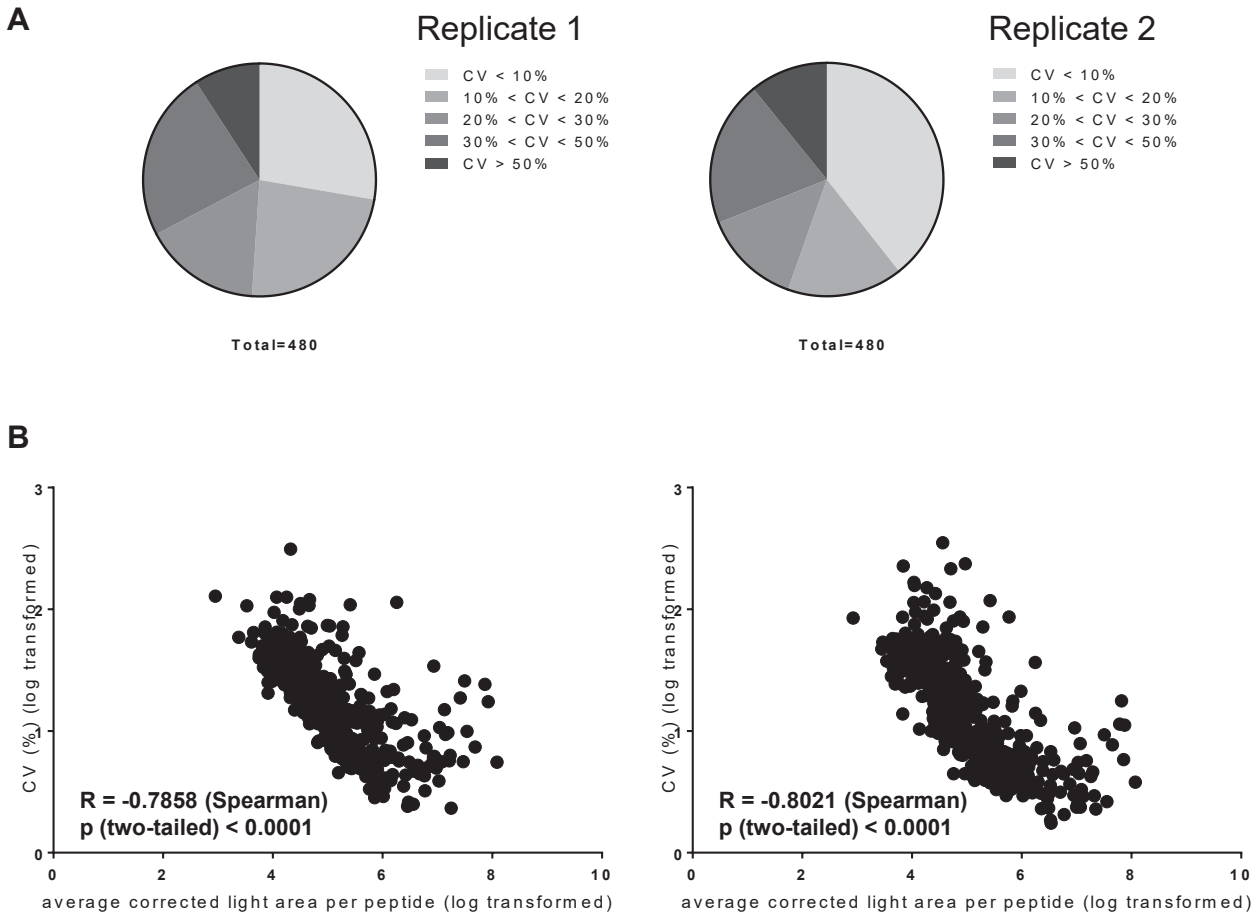

FIG. 1. **Quality controls of MRM data**. *A*, distribution of coefficient of variation (CV) across all peptides. *B*, correlation of MS signal intensity against peptide CV. MRM, multiple reaction monitoring; MS, mass spectrometry.

contrast to ESR1, the ESR2 protein is not expressed in human breast tissue.

Additional Breast Tumor Markers

LC-MRM/MS data were also obtained for other proteins of interest for breast cancer characterization: EGFR, CK5, CK14, and AR. EGFR is frequently overexpressed in TNBC and was described as a potential therapeutic target for this disease (40). In our MRM assay, EGFR was monitored using two peptides but only one of the two returned a reliable signal. Results obtained for this peptide showed significantly higher levels in TNBC samples compared to luminal A tumors ($p < 0.0001$) (Fig. 5*A*). However, this difference was not statistically significant anymore after normalization of MRM data by the tumor content (Fig. 5*C*). EGFR levels were also elevated in TNBC samples compared to HER2 tumors, but the difference was not statistically significant. A positive correlation was observed when MRM data for the EGFR peptide were plotted against the Remmele score obtained using IHC for the EGFR protein (Fig. 5, *B* and *D*).

CK5/6 and CK14 are markers of the basal breast cancer subtype, which is very similar and greatly overlaps with the triple-negative subtype (27, 29, 41). It should be noted that the antibody used for IHC measurement of CK 5/6 does not distinguish between the different human CKs 5, 6A, 6B, and 6C. In the MRM assay, CK5 (K2C5) was measured using three peptides. CK6A and CK6B were not included in the assay because the selected peptides yielded poor analytical data during assay development. For CK14 (K1C14), two peptides were initially selected but only one delivered reliable measurements. The results for the CK5 and CK14 peptides showed higher levels in TNBC compared to luminal A and HER2 tumors, but the differences were not statistically significant (supplemental Fig. S3). For both proteins, a positive correlation was observed between MRM and IHC data. CK16 (K1C16) and CK17 (K1C17) showed a similar profile as CK5 and CK14 with very low levels measured in most HER2 and luminal A samples while a wide range of concentrations was found in the TNBC group (data not shown).

AR has been reported as elevated in hormone receptor-positive tumors (42) and was also considered as a therapeutic

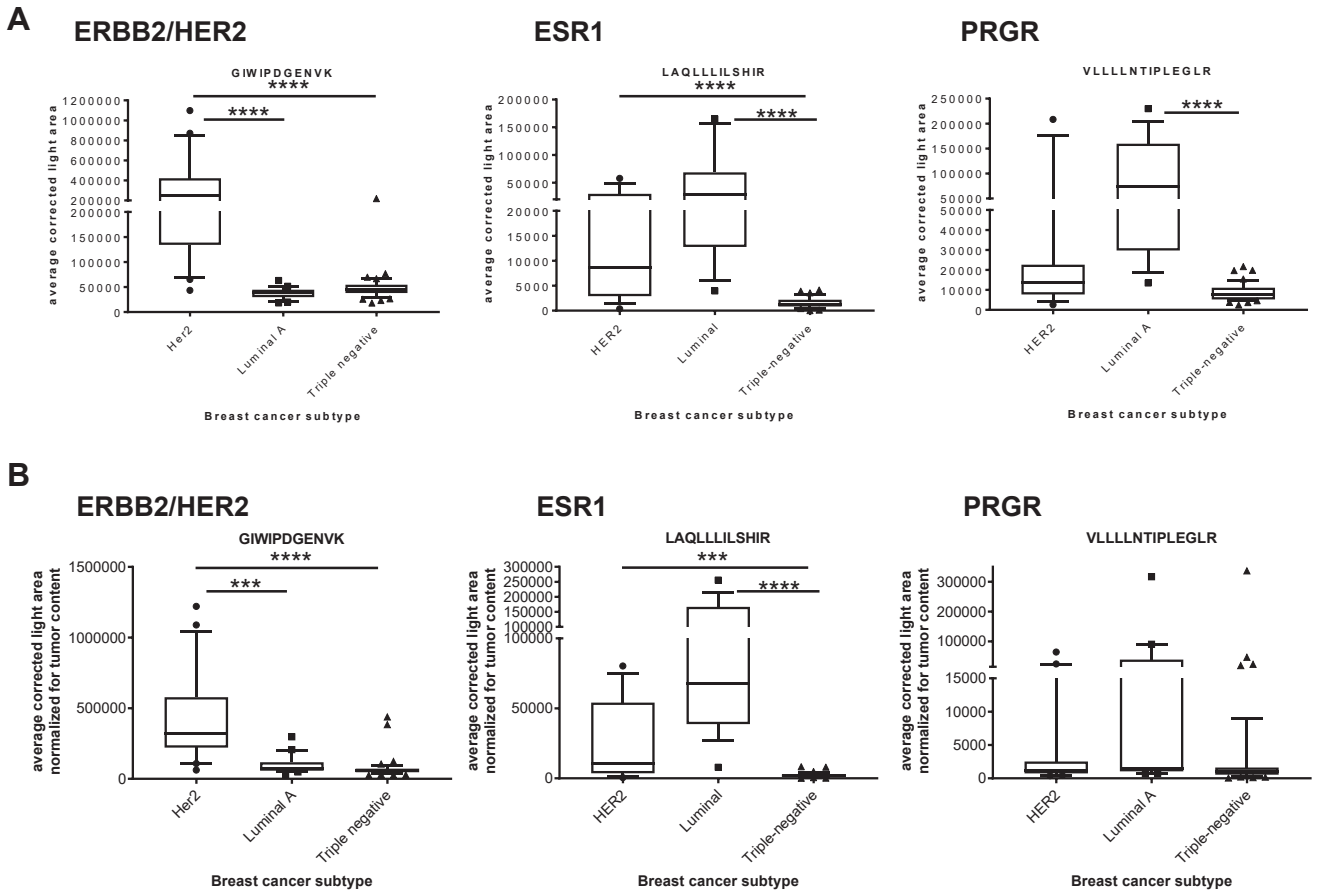

FIG. 2. **Peptide expression by MRM for the main breast cancer protein markers**. *Box plots*showing the MS signal intensity without (*A*) and with (*B*) normalization for the tumor content for the three main proteins used in the classification of breast tumors: receptor tyrosine-protein kinase erbB-2 (ERBB2/HER2), estrogen receptor (ESR1) and progesterone receptor (PRGR) (n = 88). One peptide is shown for each protein. Additional peptides are shown in the supplementary material. ERBB2 is increased in HER2 breast cancers whereas ESR1 and PRGR are increased in HER2 and luminal A cancers compared to TNBC cancers. *** indicates $p \leq 0.0007$, **** indicates $p \leq 0.0001$. MRM, multiple reaction monitoring; MS, mass spectrometry; TNBC, triple-negative breast cancer.

target in breast cancer (43). AR was monitored with three peptides in our assay but only one of them could be reliably detected. No significant difference was observed for this peptide between the three sample groups (supplemental Fig. S3).

We also measured several inflammation-related proteins using the MS assay, including CD20, CD3, and CD4. These proteins were found to be overexpressed in TNBCs and HER2 tumors compared to luminal A samples (supplemental Fig. S4). Interestingly, CD3 and CD4 showed a significant positive correlation with the level of tumor infiltrating lymphocytes (TILs) [r ranging from 0.6983 to 0.7940, p (two-tailed) < 0.0001]. CD20 showed a positive but weak correlation with TILs (r = 0.4311, p (two-tailed) < 0.0001). Interestingly, no difference in expression was observed after normalization for the tumor content. Significance of correlations was also significantly decreased. Several other proteins related to the inflammatory response, namely IFIT1, IFIT3, MX1, OASL, OAS2, and OAS3, exhibited a similar pattern of expression (supplemental Fig. S5).

Other Differentially Expressed Proteins

LC-MRM/MS analysis highlighted a number of other proteins showing a clear pattern of differential expression between the tumor groups. Among them, growth factor receptor-bound protein 7 (GRB7), a plasma membrane protein involved in the downstream signal transduction of several protein kinases, including HER2, was found to be strongly overexpressed in the group of HER2 amplified tumors (Figs. 6, *A*, *B* and S6). A significant positive correlation was observed between HER2 and GRB7 for all peptides monitored (supplemental Table S6). Another protein of interest was prolactin-inducible protein (PIP), which was significantly overexpressed in luminal A tumors compared to TNBC ($p < 0.0001$) (Figs. 6, *A*, *B* and S6).

Several proteins were identified as being frequently overexpressed in TNBC tumors compared to the other tumor groups. These proteins were measured at high levels in a large proportion of the TNBC samples, while only low amounts were detected in most, if not all, of the HER2 and luminal A tumors.

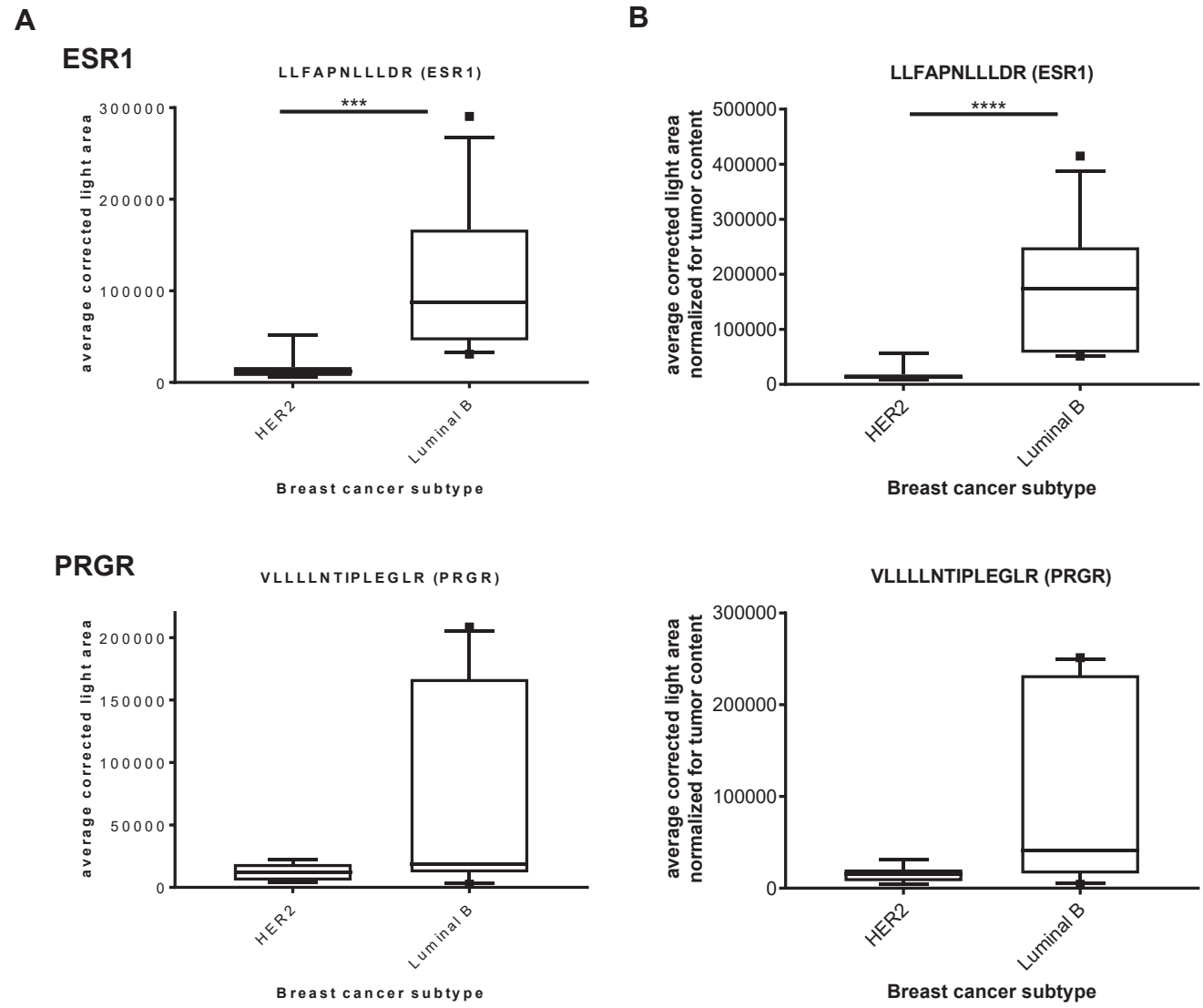

FIG. 3. **Estrogen and progesterone receptors in HER2 and luminal B tumors**. *Box plots* showing the MS signal intensity for ESR1 and PRGR peptides in HER2 tumors *versus* HER2 positive luminal B tumors without (*A*) and with (*B*) normalization for the tumor content (n = 20). *** indicates $p \leq 0.0007$, **** indicates $p \leq 0.0001$. ESR1, estrogen receptor; MS, mass spectrometry; PRGR, progesterone receptor.

A selection of proteins which showed increased expression in samples from the TNBC group is shown in Figures 7, *A*, *B* and S7. The list includes pentraxin-3 (PTX3), serpin B5/maspin, tripartite motif-containing 29 (TRI29), synemin/desmuslin, cadherin-3/P-cadherin, plakophilin-1, and phosphoserine aminotransferase (SERC). We also report proteins with decreased expression in TNBC compared to other tumors including inositol polyphosphate 4-phosphatase type II (INP4B), microtubule-associated protein tau (TAU), elastin (ELN), mucin-1 (MUC1), arylamine N-acetyltransferase 1, and melanophilin (Figs. 7, *A*, *B* and S8).

DISCUSSION

In this study, we developed multiplexed MRM methods for the analysis of a large panel of tryptic peptides extracted from FFPE breast cancer tissue samples. We obtained quantitative data for 185 proteins selected based on their known or potential association with TNBC and/or basal-like breast cancers. This represents, to our knowledge, the largest LC-MRM/MS assay developed for targeted protein measurement in FFPE tissues (12, 14, 44–47). These results are important because they indicate that despite the technical challenge represented by the sample preparation, tier two MRM assays can be developed for the relative quantification of large numbers of targeted proteins in FFPE tissue samples (48).

In this context, it was critical to show that relative changes in protein expression could be measured precisely and consistently across sample groups using the developed assays. We therefore integrated several quality checkpoints in order to control sources of potential analytical bias and

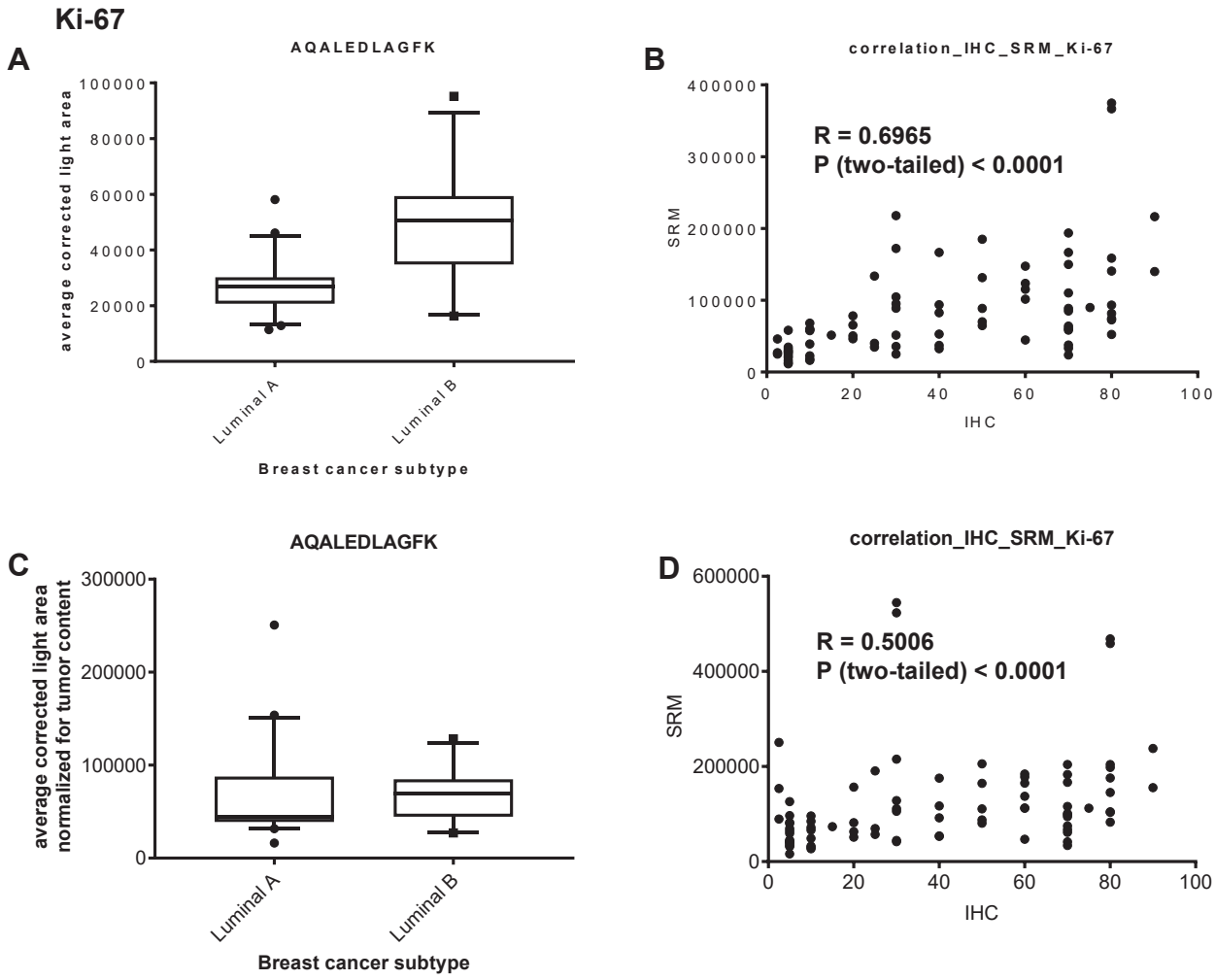

FIG. 4. **Ki-67 in luminal A and luminal B tumors**. *Box plot* showing the MS signal intensity for Ki-67 peptide in luminal A and luminal B tumors without (*A*) and with (*C*) normalization for the tumor content (n = 31). Correlation of MS signal intensity with protein expression measured by immunohistochemistry without (*B*) and with (*D*) normalization for the tumor content. Ki-67, proliferation marker protein Ki-67; MS, mass spectrometry.

achieve optimal analytical performance. The peptide extraction and the selection of peptides for the MRM assay were based on established protocols (12, 31). Variation in the amount of tumor material collected from tissue slices was taken into account in the sample preparation protocol. The goal was to obtain extracts with similar total peptide and background matrix concentrations for injection into the mass spectrometer. One of the inherent challenges with the comparative analysis of tissue samples is indeed sample size disparity. Our approach has the advantage of allowing direct result comparison after normalization by the heavy-labeled internal standards. Moreover, it also improves the reproducibility of MS analysis since ionization efficiency can be affected by the concentration of the background matrix proteins. Tumor samples were also randomized before peptide extraction and analysis in order to have a homogeneous distribution of samples from the different groups in analytical batches., In addition, a set of 12 reference peptides was used to adjust precursor acquisition windows in the MRM assay and to compensate for retention time shifts between chromatographic runs. Finally, a QC sample was used to evaluate the imprecision of MRM signals measured for all peptides during the analysis of the whole sample cohort. For the majority of proteins, we were able to monitor three proteotypic peptides per protein with three transitions per peptide, which represents a generally accepted standard for optimal analytical specificity (49, 50). However, using less than three peptides as surrogate measurement for a protein is acceptable in many cases, and adding more peptides might be needed only for measuring different isoforms of a protein.

We also included an additional level of normalization of MRM data based on the tumor content of the samples. Indeed, breast tumor biopsies consist not only of neoplastic cells but also contain multiple cell types such as fibroblasts, leukocytes, adipocytes, and myoepithelial and endothelial cells, which constitute the tumor microenvironment. The

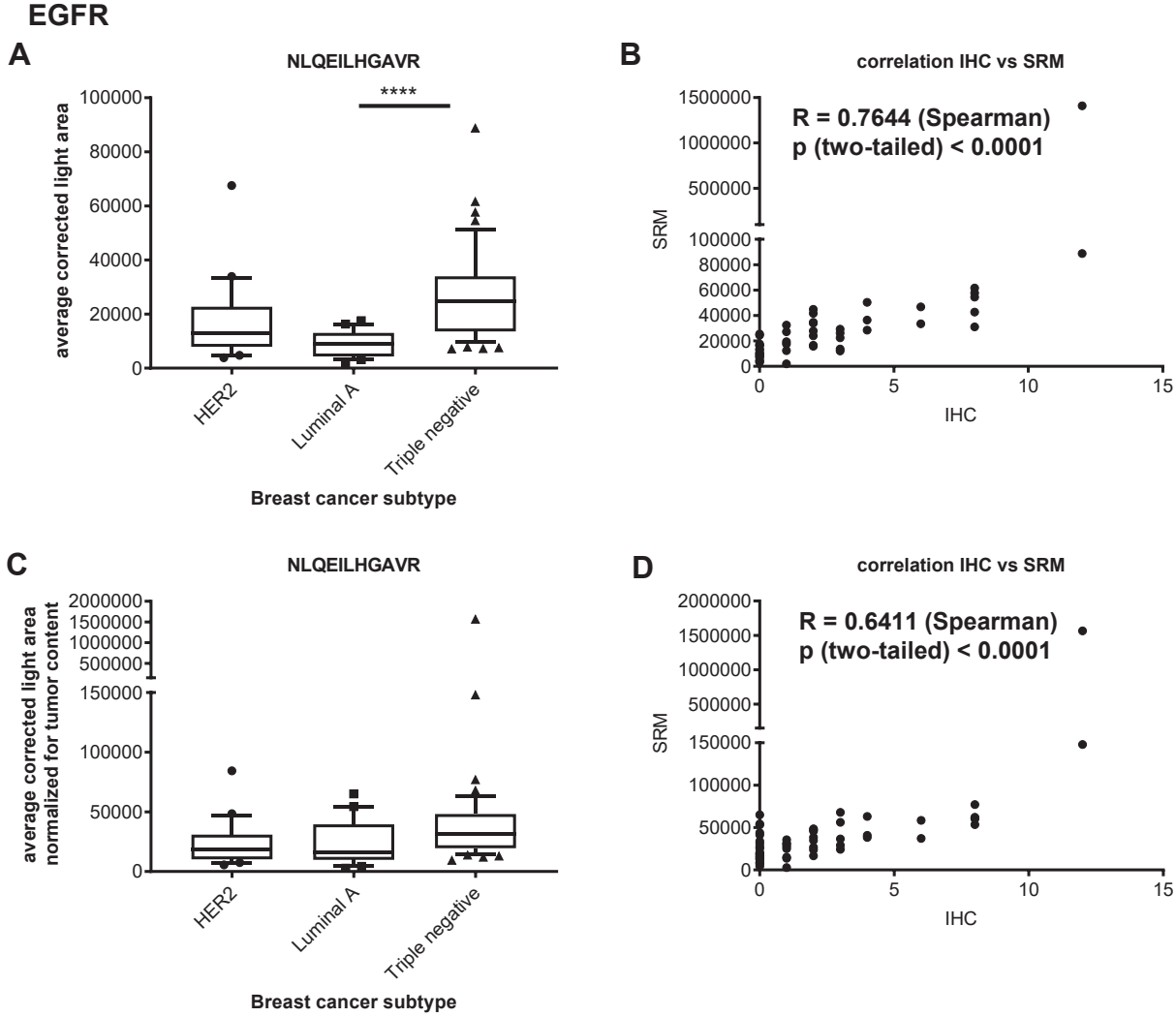

FIG. 5. **EGFR**. *Box plot* showing the MS signal intensity for epithelial growth factor receptor (EGFR) peptide in the three tumors groups without (*A*) and with (*C*) normalization for the tumor content (n = 88). Correlation of MS signal intensity with protein expression measured by immunohistochemistry without (*B*) and with (*D*) normalization for the tumor content. **** indicates $p \leq 0.0001$. EGFR, epidermal growth factor receptor; MS, mass spectrometry.

percentage of tumor cells can thus vary largely between tumor samples (from 20% to >90% in our study). This is therefore an important factor to take into account. However, the breast cancer microenvironment, including the local intratumor environment, is known to play an important role in the pathobiology of breast cancer (51) and it should not be excluded from biomarker discovery studies. Accordingly, in this work, we have considered both data with and data without normalization for the tumor content for the evaluation of protein markers. Necrosis, fibrosis, and calcification can also be found in tumor biopsies of patients that have received chemotherapy, but samples used in this work were from neoadjuvant treatment–naïve patients.

Results for proteins used in clinical pathology for breast tumor classification served as another level of confirmation that LC-MRM/MS provided reliable information. MRM data for ESR1, PRGR, and HER2 were shown to be in agreement with the corresponding IHC or CISH data and to match the classification of the HER2, luminal A, and triple-negative tumor groups. In addition, in HER2 positive tumors, MRM data were able to separate the luminal B and the HER2 tumor subgroups based on ESR1 and PRGR peptide measurement. MRM data also allowed us to distinguish luminal A from luminal B tumors based on Ki-67 peptide level. Confirmation of the reliability of LC-MRM/MS measurements also came from other proteins such as GRB7 and PIP. For GRB7, MRM results were consistent with the fact that this protein is coexpressed with HER2 in breast tumors and is involved in the same pathway (52, 53). For PIP, our findings correlated with previous research showing that this protein is increased in hormone receptor–positive breast cancer but usually not expressed in normal breast tissue (54). In that case, intermediate

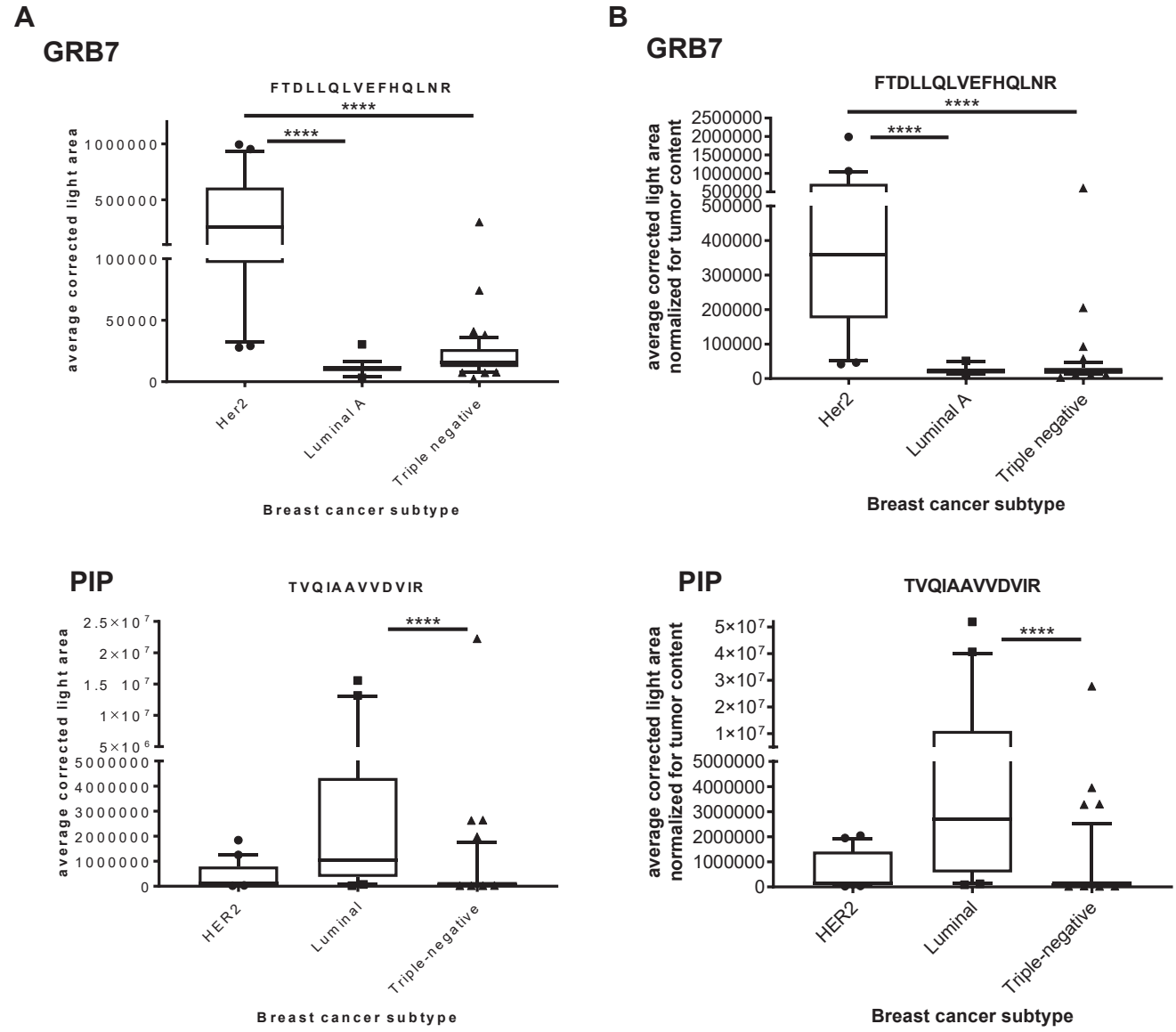

FIG. 6. **GRB7 and PIP**. *Box plots* showing the MS signal intensity for GRB7 and PIP peptides across HER2, luminal A and TNBC breast cancers without (*A*) and with (*B*) normalization for the tumor content (n = 88). **** indicates $p \leq 0.0001$. GRB7, growth factor receptor-bound protein 7; MS, mass spectrometry; PIP, prolactin-inducible protein; TNBC, triple-negative breast cancer.

expression patterns observed in HER2 overexpressing tumors for PIP can be explained by the fact that this group of samples was composed of HER2 tumors, which are hormone-receptor negative, and HER2 positive luminal B tumors, which are hormone-receptor positive.

Another interesting question was the comparison of LC-MRM/MS results with data obtained by IHC, the classical method used in clinical pathology for the assessment of protein markers expression in tissue. This was evaluated for Ki-67, EGFR, CK5, and CK14. A positive correlation was found between IHC results and MRM data for these proteins. However, the correlation was in many cases weak, which is not unexpected for two methods with highly different analytical principles. It is noteworthy that for proteins such as ER and PR, for which IHC yielded almost binary results (Remmele score of 0 or 8), LC-MRM/MS was able to provide a wide range of results. These data suggest that MRM analysis was able to distinguish fine differences in protein levels which were not necessarily reportable by IHC. In addition, for CKs, LC-MRM/MS allowed to specifically measure CK5 peptides while the antibody used for IHC cannot distinguish between human CK5 and CK6 isoforms. In contrast, we were not able to measure CK6A and CK6B by MRM since the corresponding peptides did not achieve the required analytical quality standards during assay development. This underlined the fact that IHC and LC-MRM/MS data are not directly comparable and

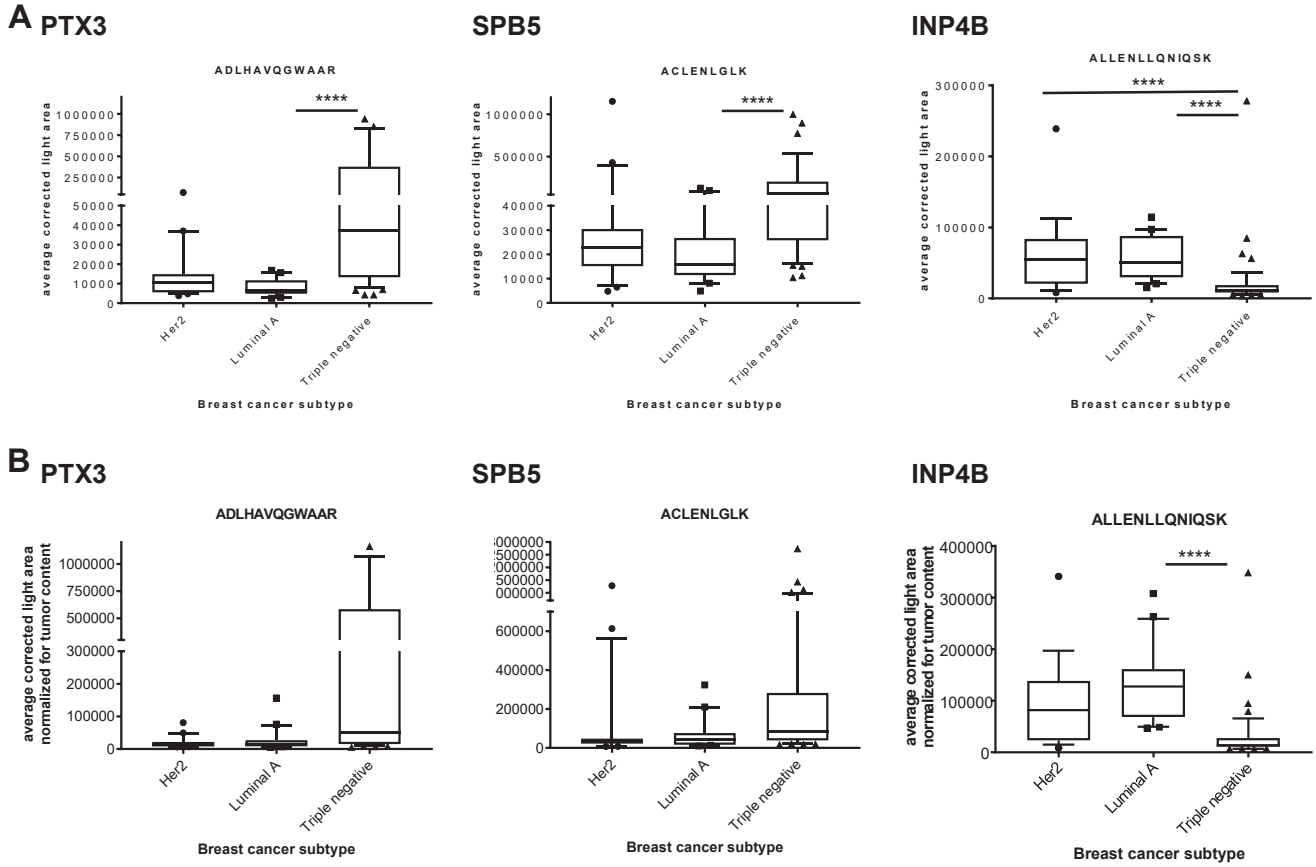

FIG. 7. **Proteins overexpressed in TNBC tumors**. *Box plots* showing the MS signal intensity for PTX3, SPB5, and INP4B peptides across HER2, luminal A, and TNBC breast cancers without (*A*) and with (*B*) normalization for the tumor content (n = 88). **** indicates $p \leq 0.0001$. INP4B, inositol polyphosphate 4-phosphatase type II; MS, mass spectrometry; SPB5, serpin B5/maspin; PTX3, pentraxin-3; TNBC, triple-negative breast cancer.

that both techniques provides complementary information on tissue protein expression. Another parameter used in clinical pathology, TILs, was found to correlate with MS data. TILs correspond to all lymphocytic cell populations that have invaded the tumor tissue. A strong correlation with TILs was observed for peptides from CD4 and CD8, which are surface markers of T lymphocytes. The correlation was weaker for CD20, a surface marker of B lymphocytes. These data are in line with the fact that most tumor infiltrating lymphocytes in breast cancers are T-cells (55). Interestingly, the differences observed between tumor groups for these proteins, as well as the correlation with TILs, were strongly decreased after normalization by the tumor content, which was fully consistent with the fact that immune cells belong to the tumor microenvironment. These results constitute a strong argument for analyzing MRM data with and without normalization by the tumor content, as previously discussed.

Since TNBC represents a group of tumors of particular interest for biomarker discovery, we also focused our attention on finding potential novel protein markers with differential expression in TNBC samples. For these proteins, we evaluated whether our results were in agreement with previous literature in order to, again, assess the reliability of MRM measurements. PTX3, SBP5, and TRI29 are proteins for which we found higher peptide levels in TNBCs compared to luminal A and HER2 tumors. PTX3 is involved in innate immunity, inflammation, and tissue repair with a potential role in various cancer processes (56), in particular in molecular pathways related to metastasis and recurrence of breast cancers (57, 58). PTX3 was identified by gene expression profiling as being differentially expressed in TNBC samples compared to luminal A, luminal B, and HER2 tumors (59). Increased expression of PTX3 was also detected in high-grade ductal infiltrating carcinomas (60) and in basal-like breast cancers where it was shown to promote stem cell-like traits and was associated with a poor prognosis (61). The second example, SBP5, is a protein with a wide range of biological activities that was described as a tumor suppressor (62, 63). However, its different roles in cancer processes are not yet clearly understood (64). Our results corroborated previous reports describing expression of SBP5 in breast cancers with aggressive phenotype, poor prognosis, and early relapse

(65–68) and in TNBC FFPE tissue samples, where it correlated with basal markers (69). TRI29 was also described as a potential tumor suppressor (70–72). In line with our results, TRI29 expression was found to be decreased in luminal A, luminal B, and HER2 tumors but not in basal-like tumors where its expression was similar to normal breast tissues (73). In contrast, peptides from INP4B, TAU, and MUC1 were found to be decreased in TNBC samples. INP4B is involved in the same signaling pathway as PTX3 and acts as a tumor suppressor by inhibiting PI3K/Akt signaling (74). Suppression of INP4B expression is a common feature in TNBC and basal-like breast cancers (75–77). For the microtubule-associated protein TAU, our results were in accordance with a study where 70% of TNBC tumors were found to be TAU negative while 75% of luminal HER2 negative and 57% of HER2 positive tumors were TAU positive (78). In addition, high TAU protein expression was identified as a prognostic factor of good outcome in breast cancer (79). The last example was MUC1, a well-known oncoprotein expressed in most breast tumors. In the literature, an association was described between ER positivity and high levels of MUC1 expression (80, 81). Other studies showed that the association with ER and PR positivity was depending on the MUC1 immunoreactivity localization pattern while negativity for MUC1 expression was associated with ER and PR negativity and the TNBC subtype (82, 83).

Proteins showing a decreased expression in the luminal A samples compared to the HER2 and TNBC groups were also identified, namely SERC, an enzyme involved in amino acid metabolism. This observation corroborates findings from a previous study where SERC was found to be upregulated in ER-negative breast cancers (84). In addition, upregulation of enzymes of the serine protease pathway was a feature observed in a majority of TNBCs, and suppression of SERC expression suggested that this protein plays a role in processes promoting metastasis (85). ELN, a protein of the extracellular matrix, had an opposite expression profile. ELN production is altered in some breast tumors leading to ELN deposition and degradation, a phenomenon called elastosis. Elastosis was found to be correlated with ER positivity in breast tumors (86–88). This feature is in agreement with the peptide expression pattern measured by MS: low levels in TNBC samples, high levels in luminal A samples, and intermediate levels in the HER2 group [the HER2 group is composed of strict HER2 breast tumors (ER and PR negative) and luminal B tumors].

Taken together, these results indicate that LC-MRM/MS is a powerful tool for the relative quantification of large numbers of candidate protein markers in FFPE tissues. In particular, the use of a targeted mass spectrometric approach to probe a finite list of targets greatly simplifies the statistical evaluation whether protein levels vary in relation to disease hallmarks. Targeted MS analysis is a highly quantitative approach, which can provide a measure for protein expression over a dynamic range of several orders of magnitude. This wide dynamic range represents a clear advantage over IHC. In this study, we used only a crude preparation of the isotopically labeled standards for cost reasons, which allowed to perform relative quantification of analytes only. Inclusion of highly purified peptides of known quantity in the MRM assay would open the way for measuring absolute concentrations of the target peptides. It would also permit MRM data comparison between laboratories. That implies however to develop and validate protocols for calibration and proper standardization when working with FFPE tissue samples. On the other hand, the method we used here only offers low spatial resolution. For this study, the entire tumor area was macrodissected, which does not provide any information on tissue and cellular distribution of the protein markers. This aspect could be improved by performing peptide extraction on subparts of the tumor or even using laser-capture microdissection but at the cost of sensitivity and assay throughput.

Based on these considerations, we believe that targeted assays based on LC-MRM/MS should be considered as a valuable screening approach for the multiplexed quantification of putative protein markers in FFPE tissue samples. Importantly, this technique enables a higher throughput testing of proteins than IHC without the additional burden of developing costly immunological reagents. The presented method provides a blueprint to select potential biomarkers, which will be confirmed in larger studies using, *e.g.*, antibody-based techniques. Such biomarker discovery pipelines will become increasingly essential to support the growing need for biomarkers in the era of Personalized Health Care.

DATA AVAILABILITY

Data can be accessed on the Panorama Public website using the following link: https://panoramaweb.org/TNBC_FFPE.url. The affiliated ProteomeXchange ID is PXD025135 (http://proteomecentral.proteomexchange.org/cgi/GetDataset?ID=PXD025135).

Supplemental data—This article contains supplemental data.

Acknowledgments—This work is dedicated to the memory of Simon McGregor. We would like to thank Tom Dunkley and Arno Friedlein for fruitful discussions around MRM assay development, Thomas McKee for valuable input on breast cancer biomarkers, Alex Scherl for running the Perl script on the peptides as well as Jens Lamerz for his input on statistical data analysis.

Author contributions—C. S., P. L., P. C., and A. D. conceptualization; C. S., P. L., P. C., J.-C. T., and A. D. methodology; C. S. validation; C. S. and J.-C. T. formal analysis; C. S. data curation; C. S. and P. L. writing-original draft; C. S., P. L., P. C., J.-C. T., and A. D. writing-review &

editing; C. S. and P. L. visualization; C. S. project administration; P. L., A. D., and P. C. supervision; P. L., A. D., and P. C. funding acquisition; J.-C. T. resources.

Funding and additional information—C. S. was supported by a Roche Postdoctoral Fellowship.

Conflict of interest—The authors declare no competing interests.

Abbreviations—The abbreviations used are: AR, androgen receptor; CV, coefficient of variation; CK, cytokeratin; CISH, chromogenic *in situ* hybridization; ER, estrogen receptor; EGFR, epidermal growth factor receptor; FFPE, formalin-fixed paraffin-embedded; H&E, hematoxylin and eosin; IHC, immunohistochemistry; Ki-67, proliferation marker protein Ki-67; LC-MRM/MS, liquid chromatography coupled to multiple reaction monitoring spectrometry; MRM, multiple reaction monitoring; MS, mass spectrometry; PR, progesterone receptor; TILs, tumor infiltrating lymphocytes; TNBC, triple-negative breast cancer.

Received December 16, 2021, and in revised form, September 15, 2022 Published, MCPRO Papers in Press, September 22, 2022, https://doi.org/10.1016/j.mcpro.2022.100416

REFERENCES

1. Szasz, A. M., Gyorffy, B., and Marko-Varga, G. (2017) Cancer heterogeneity determined by functional proteomics. *Semin. Cell Dev. Biol.* **64**, 132–142
2. Matboli, M., El-Nakeep, S., Hossam, N., Habieb, A., Azazy, A. E., Ebrahim, A. E., *et al*. (2016) Exploring the role of molecular biomarkers as a potential weapon against gastric cancer: a review of the literature. *World J. Gastroenterol.* **22**, 5896–5908
3. Barbieri, C. E., Chinnaiyan, A. M., Lerner, S. P., Swanton, C., and Rubin, M. A. (2017) The emergence of precision urologic oncology: a collaborative review on biomarker-driven therapeutics. *Eur. Urol.* **71**, 237–246
4. Hinestrosa, M. C., Dickersin, K., Klein, P., Mayer, M., Noss, K., Slamon, D., *et al*. (2007) Shaping the future of biomarker research in breast cancer to ensure clinical relevance. *Nat. Rev. Cancer* **7**, 309–315
5. Perez-Gracia, J. L., Sanmamed, M. F., Bosch, A., Patino-Garcia, A., Schalper, K. A., Segura, V., *et al*. (2017) Strategies to design clinical studies to identify predictive biomarkers in cancer research. *Cancer Treat Rev.* **53**, 79–97
6. Ikeda, K., Monden, T., Kanoh, T., Tsujie, M., Izawa, H., Haba, A., *et al*. (1998) Extraction and analysis of diagnostically useful proteins from formalin-fixed, paraffin-embedded tissue sections. *J. Histochem. Cytochem.* **46**, 397–403
7. Hood, B. L., Conrads, T. P., and Veenstra, T. D. (2006) Mass spectrometric analysis of formalin-fixed paraffin-embedded tissue: unlocking the proteome within. *Proteomics* **6**, 4106–4114
8. Vincenti, D. C., and Murray, G. I. (2013) The proteomics of formalin-fixed wax-embedded tissue. *Clin. Biochem.* **46**, 546–551
9. Giusti, L., and Lucacchini, A. (2013) Proteomic studies of formalin-fixed paraffin-embedded tissues. *Exp. Rev. Proteomics* **10**, 165–177
10. Nuciforo, P., Thyparambil, S., Aura, C., Garrido-Castro, A., Vilaro, M., Peg, V., *et al*. (2016) High HER2 protein levels correlate with increased survival in breast cancer patients treated with anti-HER2 therapy. *Mol. Oncol.* **10**, 138–147
11. Catenacci, D. V., Liao, W. L., Thyparambil, S., Henderson, L., Xu, P., Zhao, L., *et al*. (2014) Absolute quantitation of met using mass spectrometry for clinical application: assay precision, stability, and correlation with MET gene amplification in FFPE tumor tissue. *PLoS One* **9**, e100586
12. Hembrough, T., Thyparambil, S., Liao, W. L., Darfler, M. M., Abdo, J., Bengali, K. M., *et al*. (2013) Application of selected reaction monitoring for multiplex quantification of clinically validated biomarkers in formalin-fixed, paraffin-embedded tumor tissue. *J. Mol. Diagn.* **15**, 454–465
13. Steiner, C., Tille, J. C., Lamerz, J., Kux van Geijtenbeek, S., McKee, T. A., Venturi, M., *et al*. (2015) Quantification of HER2 by targeted mass spectrometry in formalin-fixed paraffin-embedded (FFPE) breast cancer tissues. *Mol. Cell Proteomics* **14**, 2786–2799
14. Catenacci, D. V. T., Liao, W. L., Zhao, L., Whitcomb, E., Henderson, L., O'Day, E., *et al*. (2016) Mass-spectrometry-based quantitation of Her2 in gastroesophageal tumor tissue: comparison to IHC and FISH. *Gastric Cancer* **19**, 1066–1079
15. Foulkes, W. D., Smith, I. E., and Reis-Filho, J. S. (2010) Triple-negative breast cancer. *N. Engl. J. Med.* **363**, 1938–1948
16. Reis-Filho, J. S., and Tutt, A. N. (2008) Triple negative tumours: a critical review. *Histopathology* **52**, 108–118
17. Boyle, P. (2012) Triple-negative breast cancer: epidemiological considerations and recommendations. *Ann. Oncol.* **23**, vi7–vi12
18. Brenton, J. D., Carey, L. A., Ahmed, A. A., and Caldas, C. (2005) Molecular classification and molecular forecasting of breast cancer: ready for clinical application? *J. Clin. Oncol.* **23**, 7350–7360
19. Barnard, M. E., Boeke, C. E., and Tamimi, R. M. (2015) Established breast cancer risk factors and risk of intrinsic tumor subtypes. *Biochim. Biophys. Acta* **1856**, 73–85
20. Wahba, H. A., and El-Hadaad, H. A. (2015) Current approaches in treatment of triple-negative breast cancer. *Cancer Biol. Med.* **12**, 106–116
21. Marme, F., and Schneeweiss, A. (2015) Targeted therapies in triple-negative breast cancer. *Breast Care (Basel)* **10**, 159–166
22. Mustacchi, G., and De Laurentiis, M. (2015) The role of taxanes in triple-negative breast cancer: literature review. *Drug Des. Dev. Ther.* **9**, 4303–4318
23. Lehmann, B. D., and Pietenpol, J. A. (2015) Clinical implications of molecular heterogeneity in triple negative breast cancer. *Breast* **24**, S36–40
24. Perou, C. M., Sorlie, T., Eisen, M. B., van de Rijn, M., Jeffrey, S. S., Rees, C. A., *et al*. (2000) Molecular portraits of human breast tumours. *Nature* **406**, 747–752
25. Parker, J. S., Mullins, M., Cheang, M. C., Leung, S., Voduc, D., Vickery, T., *et al*. (2009) Supervised risk predictor of breast cancer based on intrinsic subtypes. *J. Clin. Oncol.* **27**, 1160–1167
26. Sorlie, T., Perou, C. M., Tibshirani, R., Aas, T., Geisler, S., Johnsen, H., *et al*. (2001) Gene expression patterns of breast carcinomas distinguish tumor subclasses with clinical implications. *Proc. Natl. Acad. Sci. U. S. A.* **98**, 10869–10874
27. Smid, M., Wang, Y., Zhang, Y., Sieuwerts, A. M., Yu, J., Klijn, J. G., *et al*. (2008) Subtypes of breast cancer show preferential site of relapse. *Cancer Res.* **68**, 3108–3114
28. O'Toole, S. A., Beith, J. M., Millar, E. K., West, R., McLean, A., Cazet, A., *et al*. (2013) Therapeutic targets in triple negative breast cancer. *J. Clin. Pathol.* **66**, 530–542
29. Rody, A., Karn, T., Liedtke, C., Pusztai, L., Ruckhaeberle, E., Hanker, L., *et al*. (2011) A clinically relevant gene signature in triple negative and basal-like breast cancer. *Breast Cancer Res.* **13**, R97
30. Liu, N. Q., Stingl, C., Look, M. P., Smid, M., Braakman, R. B., De Marchi, T., *et al*. (2014) Comparative proteome analysis revealing an 11-protein signature for aggressive triple-negative breast cancer. *J. Natl. Cancer Inst.* **106**, djt376
31. Steiner, C., Lescuyer, P., Tille, J. C., Cutler, P., and Ducret, A. (2019) Development of a highly multiplexed SRM assay for biomarker discovery in formalin-fixed paraffin-embedded tissues. *Met. Mol. Biol.* **1959**, 185–203
32. Scherl, A., Shaffer, S. A., Taylor, G. K., Kulasekara, H. D., Miller, S. I., and Goodlett, D. R. (2008) Genome-specific gas-phase fractionation strategy for improved shotgun proteomic profiling of proteotypic peptides. *Anal. Chem.* **80**, 1182–1191
33. Escher, C., Reiter, L., MacLean, B., Ossola, R., Herzog, F., Chilton, J., *et al*. (2012) Using iRT, a normalized retention time for more targeted measurement of peptides. *Proteomics* **12**, 1111–1121
34. Gallien, S., Peterman, S., Kiyonami, R., Souady, J., Duriez, E., Schoen, A., *et al*. (2012) Highly multiplexed targeted proteomics using precise control of peptide retention time. *Proteomics* **12**, 1122–1133
35. Kiyonami, R., Schoen, A., Prakash, A., Nguyen, H., Peterman, S., Selevsek, N., *et al*. (2009) Rapid assay development and refinement for targeted

protein quantitation using an intelligent SRM (iSRM) workflow. *Thermo Sci. Appl. Note* **468**, 1–12
36. Maclean, B., Tomazela, D. M., Abbatiello, S. E., Zhang, S., Whiteaker, J. R., Paulovich, A. G., *et al*. (2010) Effect of collision energy optimization on the measurement of peptides by selected reaction monitoring (SRM) mass spectrometry. *Anal. Chem.* **82**, 10116–10124
37. Sharma, V., Eckels, J., Taylor, G. K., Shulman, N. J., Stergachis, A. B., Joyner, S. A., *et al*. (2014) Panorama: a targeted proteomics knowledge base. *J. Proteome Res.* **13**, 4205–4210
38. Dunkley, T., Costa, V., Friedlein, A., Lugert, S., Aigner, S., Ebeling, M., *et al*. (2015) Characterization of a human pluripotent stem cell-derived model of neuronal development using multiplexed targeted proteomics. *Proteomics Clin. Appl.* **9**, 684–694
39. Goldhirsch, A., Winer, E. P., Coates, A. S., Gelber, R. D., Piccart-Gebhart, M., Thurlimann, B., *et al*. (2013) Personalizing the treatment of women with early breast cancer: highlights of the St gallen international expert consensus on the primary therapy of early breast cancer 2013. *Ann. Oncol.* **24**, 2206–2223
40. Nakai, K., Hung, M. C., and Yamaguchi, H. (2016) A perspective on anti-EGFR therapies targeting triple-negative breast cancer. *Am. J. Cancer Res.* **6**, 1609–1623
41. Lachapelle, J., and Foulkes, W. D. (2011) Triple-negative and basal-like breast cancer: implications for oncologists. *Curr. Oncol.* **18**, 161–164
42. Kensler, K. H., Regan, M. M., Heng, Y. J., Baker, G. M., Pyle, M. E., Schnitt, S. J., *et al*. (2019) Prognostic and predictive value of androgen receptor expression in postmenopausal women with estrogen receptor-positive breast cancer: results from the breast international group trial 1-98. *Breast Cancer Res.* **21**, 30
43. Caswell-Jin, J. L., and Curtis, C. (2021) Androgen receptor agonists as breast cancer therapeutics. *Nat. Med.* **27**, 198–199
44. Trapphoff, T., Heiligentag, M., Dankert, D., Demond, H., Deutsch, D., Frohlich, T., *et al*. (2016) Postovulatory aging affects dynamics of mRNA, expression and localization of maternal effect proteins, spindle integrity and pericentromeric proteins in mouse oocytes. *Hum. Reprod.* **31**, 133–149
45. Sprung, R. W., Martinez, M. A., Carpenter, K. L., Ham, A. J., Washington, M. K., Arteaga, C. L., *et al*. (2012) Precision of multiple reaction monitoring mass spectrometry analysis of formalin-fixed, paraffin-embedded tissue. *J. Proteome Res.* **11**, 3498–3505
46. Gamez-Pozo, A., Sanchez-Navarro, I., Calvo, E., Diaz, E., Miguel-Martin, M., Lopez, R., *et al*. (2011) Protein phosphorylation analysis in archival clinical cancer samples by shotgun and targeted proteomics approaches. *Mol. Biosyst.* **7**, 2368–2374
47. Park, J., Oh, H. J., Han, D., Wang, J. I., Park, I. A., Ryu, H. S., *et al*. (2020) Parallel reaction monitoring-mass spectrometry (PRM-MS)-Based targeted proteomic surrogates for intrinsic subtypes in breast cancer: comparative analysis with immunohistochemical phenotypes. *J. Proteome Res.* **19**, 2643–2653
48. Carr, S. A., Abbatiello, S. E., Ackermann, B. L., Borchers, C., Domon, B., Deutsch, E. W., *et al*. (2014) Targeted peptide measurements in biology and medicine: best practices for mass spectrometry-based assay development using a fit-for-purpose approach. *Mol. Cell Proteomics* **13**, 907–917
49. Lange, V., Picotti, P., Domon, B., and Aebersold, R. (2008) Selected reaction monitoring for quantitative proteomics: a tutorial. *Mol. Syst. Biol.* **4**, 222
50. Gallien, S., Duriez, E., and Domon, B. (2011) Selected reaction monitoring applied to proteomics. *J. Mass Spectrom.* **46**, 298–312
51. Soysal, S. D., Tzankov, A., and Muenst, S. E. (2015) Role of the tumor microenvironment in breast cancer. *Pathobiology* **82**, 142–152
52. Stein, D., Wu, J., Fuqua, S. A., Roonprapunt, C., Yajnik, V., D'Eustachio, P., *et al*. (1994) The SH2 domain protein GRB-7 is co-amplified, overexpressed and in a tight complex with HER2 in breast cancer. *EMBO J.* **13**, 1331–1340
53. Janes, P. W., Lackmann, M., Church, W. B., Sanderson, G. M., Sutherland, R. L., and Daly, R. J. (1997) Structural determinants of the interaction between the erbB2 receptor and the Src homology 2 domain of Grb7. *J. Biol. Chem.* **272**, 8490–8497
54. Ihedioha, O., Blanchard, A. A., Balhara, J., Okwor, I., Jia, P., Uzonna, J., *et al*. (2018) The human breast cancer-associated protein, the prolactin-inducible protein (PIP), regulates intracellular signaling events and cytokine production by macrophages. *Immunol. Res.* **66**, 245–254
55. Savas, P., Salgado, R., Denkert, C., Sotiriou, C., Darcy, P. K., Smyth, M. J., *et al*. (2016) Clinical relevance of host immunity in breast cancer: from TILs to the clinic. *Nat. Rev. Clin. Oncol.* **13**, 228–241
56. Giacomini, A., Ghedini, G. C., Presta, M., and Ronca, R. (2018) Long pentraxin 3: a novel multifaceted player in cancer. *Biochim. Biophys. Acta Rev. Cancer* **1869**, 53–63
57. Wills, C. A., Liu, X., Chen, L., Zhao, Y., Dower, C. M., Sundstrom, J., *et al*. (2021) Chemotherapy-induced upregulation of small extracellular vesicle-associated PTX3 accelerates breast cancer metastasis. *Cancer Res.* **81**, 452–463
58. Zhang, P., Liu, Y., Lian, C., Cao, X., Wang, Y., Li, X., *et al*. (2020) SH3RF3 promotes breast cancer stem-like properties *via* JNK activation and PTX3 upregulation. *Nat. Commun.* **11**, 2487
59. Player, A., Abraham, N., Burrell, K., Bengone, I. O., Harris, A., Nunez, L., *et al*. (2017) Identification of candidate genes associated with triple negative breast cancer. *Genes Cancer* **8**, 659–672
60. Scimeca, M., Antonacci, C., Colombo, D., Bonfiglio, R., Buonomo, O. C., and Bonanno, E. (2016) Emerging prognostic markers related to mesenchymal characteristics of poorly differentiated breast cancers. *Tumour Biol.* **37**, 5427–5435
61. Thomas, C., Robinson, C., Dessauvagie, B., Wood, B., Sterrett, G., Harvey, J., *et al*. (2017) Expression of proliferation genes in formalin-fixed paraffin-embedded (FFPE) tissue from breast carcinomas. Feasibility and relevance for a routine histopathology laboratory. *J. Clin. Pathol.* **70**, 25–32
62. Zou, Z., Anisowicz, A., Hendrix, M. J., Thor, A., Neveu, M., Sheng, S., *et al*. (1994) Maspin, a serpin with tumor-suppressing activity in human mammary epithelial cells. *Science* **263**, 526–529
63. Seftor, R. E., Seftor, E. A., Sheng, S., Pemberton, P. A., Sager, R., and Hendrix, M. J. (1998) Maspin suppresses the invasive phenotype of human breast carcinoma. *Cancer Res.* **58**, 5681–5685
64. Bernardo, M. M., Dzinic, S. H., Matta, M. J., Dean, I., Saker, L., and Sheng, S. (2017) The opportunity of precision medicine for breast cancer with context-sensitive tumor suppressor maspin. *J. Cell Biochem.* **118**, 1639–1647
65. Umekita, Y., Ohi, Y., Sagara, Y., and Yoshida, H. (2002) Expression of maspin predicts poor prognosis in breast-cancer patients. *Int. J. Cancer* **100**, 452–455
66. Umekita, Y., and Yoshida, H. (2003) Expression of maspin is up-regulated during the progression of mammary ductal carcinoma. *Histopathology* **42**, 541–545
67. Joensuu, K. M., Leidenius, M. H., Andersson, L. C., and Heikkila, P. S. (2009) High expression of maspin is associated with early tumor relapse in breast cancer. *Hum. Pathol.* **40**, 1143–1151
68. Kim, D. H., Yoon, D. S., Dooley, W. C., Nam, E. S., Ryu, J. W., Jung, K. C., *et al*. (2003) Association of maspin expression with the high histological grade and lymphocyte-rich stroma in early-stage breast cancer. *Histopathology* **42**, 37–42
69. Umekita, Y., Ohi, Y., Souda, M., Rai, Y., Sagara, Y., Sagara, Y., *et al*. (2011) Maspin expression is frequent and correlates with basal markers in triple-negative breast cancer. *Diagn. Pathol.* **6**, 36
70. Liu, J., Welm, B., Boucher, K. M., Ebbert, M. T., and Bernard, P. S. (2012) TRIM29 functions as a tumor suppressor in nontumorigenic breast cells and invasive ER+ breast cancer. *Am. J. Pathol.* **180**, 839–847
71. Ai, L., Kim, W. J., Alpay, M., Tang, M., Pardo, C. E., Hatakeyama, S., *et al*. (2014) TRIM29 suppresses TWIST1 and invasive breast cancer behavior. *Cancer Res.* **74**, 4875–4887
72. Yanagi, T., Watanabe, M., Hata, H., Kitamura, S., Imafuku, K., Yanagi, H., *et al*. (2018) Loss of TRIM29 alters keratin distribution to promote cell invasion in squamous cell carcinoma. *Cancer Res.* **78**, 6795–6806
73. Avraham, A., Cho, S. S., Uhlmann, R., Polak, M. L., Sandbank, J., Karni, T., *et al*. (2014) Tissue specific DNA methylation in normal human breast epithelium and in breast cancer. *PLoS One* **9**, e91805
74. Fedele, C. G., Ooms, L. M., Ho, M., Vieusseux, J., O'Toole, S. A., Millar, E. K., *et al*. (2010) Inositol polyphosphate 4-phosphatase II regulates PI3K/Akt signaling and is lost in human basal-like breast cancers. *Proc. Natl. Acad. Sci. U. S. A.* **107**, 22231–22236
75. Liu, H., Paddock, M. N., Wang, H., Murphy, C. J., Geck, R. C., Navarro, A. J., *et al*. (2020) The INPP4B tumor suppressor modulates EGFR trafficking and promotes triple-negative breast cancer. *Cancer Discov.* **10**, 1226–1239

76. Lehmann, B. D., Bauer, J. A., Schafer, J. M., Pendleton, C. S., Tang, L., Johnson, K. C., *et al*. (2014) PIK3CA mutations in androgen receptor-positive triple negative breast cancer confer sensitivity to the combination of PI3K and androgen receptor inhibitors. *Breast Cancer Res.* **16**, 406
77. Won, J. R., Gao, D., Chow, C., Cheng, J., Lau, S. Y., Ellis, M. J., *et al*. (2013) A survey of immunohistochemical biomarkers for basal-like breast cancer against a gene expression profile gold standard. *Mod. Pathol.* **26**, 1438–1450
78. Lei, C., Yang, C., Xia, B., Ji, F., Zhang, Y., Gao, H., *et al*. (2020) Analysis of tau protein expression in predicting pathological complete response to neoadjuvant chemotherapy in different molecular subtypes of breast cancer. *J. Breast Cancer* **23**, 47–58
79. Bonneau, C., Gurard-Levin, Z. A., Andre, F., Pusztai, L., and Rouzier, R. (2015) Predictive and prognostic value of the TauProtein in breast cancer. *Anticancer Res.* **35**, 5179–5184
80. McGuckin, M. A., Walsh, M. D., Hohn, B. G., Ward, B. G., and Wright, R. G. (1995) Prognostic significance of MUC1 epithelial mucin expression in breast cancer. *Hum. Pathol.* **26**, 432–439
81. Rakha, E. A., Boyce, R. W., Abd El-Rehim, D., Kurien, T., Green, A. R., Paish, E. C., *et al*. (2005) Expression of mucins (MUC1, MUC2, MUC3, MUC4, MUC5AC and MUC6) and their prognostic significance in human breast cancer. *Mod. Pathol.* **18**, 1295–1304
82. van der Vegt, B., de Roos, M. A., Peterse, J. L., Patriarca, C., Hilkens, J., de Bock, G. H., *et al*. (2007) The expression pattern of MUC1 (EMA) is related to tumour characteristics and clinical outcome of invasive ductal breast carcinoma. *Histopathology* **51**, 322–335
83. Iizuka, M., Nakanishi, Y., Fuchinoue, F., Maeda, T., Murakami, E., Obana, Y., *et al*. (2015) Altered intracellular region of MUC1 and disrupted correlation of polarity-related molecules in breast cancer subtypes. *Cancer Sci.* **106**, 307–314
84. Gao, S., Ge, A., Xu, S., You, Z., Ning, S., Zhao, Y., *et al*. (2017) PSAT1 is regulated by ATF4 and enhances cell proliferation *via* the GSK3beta/beta-catenin/cyclin D1 signaling pathway in ER-negative breast cancer. *J. Exp. Clin. Cancer Res.* **36**, 179
85. Metcalf, S., Dougherty, S., Kruer, T., Hasan, N., Biyik-Sit, R., Reynolds, L., *et al*. (2020) Selective loss of phosphoserine aminotransferase 1 (PSAT1) suppresses migration, invasion, and experimental metastasis in triple negative breast cancer. *Clin. Exp. Metastasis* **37**, 187–197
86. Tosi, P., Baak, J. P., Luzi, P., Sforza, V., Santopietro, R., and Lio, R. (1987) Correlation between immunohistochemically determined oestrogen receptor content, using monoclonal antibodies, and qualitative and quantitative tissue features in ductal breast cancer. *Histopathology* **11**, 741–751
87. Giri, D. D., Lonsdale, R. N., Dangerfield, V. J., Harris, S. C., Parsons, M. A., and Underwood, J. C. (1987) Clinicopathological significance of intratumoural variations in elastosis grades and the oestrogen receptor status of human breast carcinomas. *J. Pathol.* **151**, 297–303
88. Kadar, A., Tokes, A. M., Kulka, J., and Robert, L. (2002) Extracellular matrix components in breast carcinomas. *Semin. Cancer Biol.* **12**, 243–257